HIGHLIGHTED PAPER

Physical, mechanical, and microstructural characterization of novel, 3D-printed, tunable, lab-grown plant materials generated from *Zinnia elegans* cell cultures

Ashley L. Beckwith [1,2,†], Jeffrey T. Borenstein [2,‡], Luis F. Velásquez-García [3,*]

[1] Mechanical Engineering, Massachusetts Institute of Technology, Cambridge, MA, USA
[2] Charles Stark Draper Laboratory, Cambridge, MA, USA
[3] Microsystems Technology Laboratories, Massachusetts Institute of Technology, Cambridge, MA, USA

To date, wood has been viewed as an attractive commodity because of its low relative cost and widespread availability. However, supply is increasingly strained, and, in many ways, trees make a non-ideal feedstock—with slow, climate and seasonally dependent growth, low yields of high-value products, and susceptibility to pests and disease. Recent research offered an approach to generate plant-based materials *in vitro* without needing to harvest or process whole plants, thereby enabling: localized, high-density production, elimination of energy-intensive collection and hauling, reduced processing, and inherent climate resilience. This work reports the first physical, mechanical, and microstructural characterization of 3-D printed, lab-grown, and tunable plant materials generated with *Zinnia elegans* cell cultures using such methodology. The data show that the properties of the resulting plant materials vary significantly with adjustments to hormone levels present in growth medium. In addition, configuration of the culture environment via bioprinting and casting enables the production of net-shape materials in forms and scales that do not arise naturally in whole plants. Finally, new comparative data on cell development in response to hormone levels in culture medium demonstrates the repeatability of growth trends, clarifies the relationship between developmental pathways, and helps to elucidate the relationships between cellular-level culture characteristics and emergent material properties.

Keywords: Agriculture; Bioprinting; Cell culture; Lab-grown; Plant material; Wood

Introduction

Research shows that deforestation, forest management, and change of land use causes a net loss of as many as 15.3 billion trees per year [11]; if current consumption rates continue, some researchers predict that all the world's forests could disappear in as little as 100 to 200 years[6]. The increasingly strained wood supply is exacerbated by the naturally slow growth of trees[2], relatively low yields of high-value materials[7], and waste associated with tree harvest, transport, and processing. Meanwhile, demand for plant-based materials, e.g., wood, continues to grow as environmentally conscious markets seek alternatives to fossil-fuel derived products[25]. Solutions are urgently needed to support the growing demand for wood and other plant-based products while simultaneously counteracting trends in deforestation and loss of biodiversity with land conversion to monocultural plantations.

Recent work proposed a novel approach to generate 3D-printed, tunable plant materials from cell cultures with the potential to reduce waste, increase yields and production rates,

* Corresponding author at: 60 Vassar St, Cambridge, MA 02139, USA.
E-mail addresses: Beckwith, A.L. (ashbeck@mit.edu), Borenstein, J.T. (jborenstein@draper.com), Velásquez-García, L.F. (Velasquez@alum.mit.edu).
† 77 Massachusetts Ave, Cambridge, MA 02139, USA.
‡ 555 Technology Square, Cambridge, MA 02139 USA.

https://doi.org/10.1016/j.mattod.2022.02.012

and reduce environmental disruption as cultures are generated from a non-sacrificial plant sample rather than whole plants[3]; using a *Zinnia elegans* model, the authors provided the first proof-of-concept demonstration of such methodology. The reported experiments demonstrated that plant cell populations within a hydrogel growth environment could be directed to present varied cell types and morphologies by modifying controllable inputs such as hormone concentrations, pH, and cell density [3]. An understanding of the relationship between cellular properties in the living culture and the corresponding attributes in the resulting material product is necessary to direct the growth of materials with targeted physical characteristics, but this knowledge had not yet been established. Using *Zinnia elegans* cell cultures, this work reports the first physical, mechanical, and microstructural characterization of plant materials generated by the proposed selective-growth method, helping elucidate the relationships between cellular-level culture characteristics and emergent material properties.

In principle, the effort to produce plant materials in the absence of the supporting plant is not entirely unlike tissue engineering in animal cell systems. In both fields, cells in a structured, nutrient-rich growth environment can be directed to grow and transform into tissue-like products. The primary differences lie in the specifics of execution. Compared with animal cell types, plant cells employ different metabolic pathways, require distinct growth inputs and environments, and rely on specialized developmental signals to drive development into desired cell types. Regardless of these dissimilarities between *in vitro* mammalian and plant tissue generation, historical insights from the more-developed mammalian field can be useful for contextualizing and predicting a trajectory for grown-to-order plant materials.

Tissue engineering is a complex, interdisciplinary field requiring knowledge on the impacts of numerous interactive factors on growth and development of individual cells and tissues[4]. To mimic tissue growth *in vitro*, both living components (i.e., cells) and interactions with their non-living surroundings (i.e., culture environment, scaffolding, etc.) must be taken into account. Decades of work is often undertaken to establish the resolution of knowledge required to precisely coordinate cellular behavior. Early tissue engineering efforts focused on generating skin replacements, and a simple, two-layer living composite was demonstrated nearly two decades after conceptualization [4]. Work towards the production of more complex tissues like cardiac muscle has been on-going for closer to four decades [18,10]. Today, principles in tissue engineering are being leveraged to produce food products, in a practice known as cellular agriculture[26]. Modern cellular agriculture efforts promise to selectively generate meat products (i.e., tissues or tissue-like agglomerations) without sacrificing any animals, with the motivation of circumventing morally and environmentally dubious practices associated with standard meat production. The presented effort to selectively produce plant materials, like cellular agriculture, aims to use resources more efficiently and localize production of goods to reduce environmental impacts.

To date, tissue engineering efforts have almost entirely focused on animal cell culture. Analogous concepts have not been translated to the plant culture space, particularly with respect to the production of materials. This work thus represents a first look at a cellular agriculture approach to plant material generation.

This report is divided into three parts that provide new insights on cellular-level tunability, culture-scale and form control, and the physical, mechanical, and microstructural characteristics of the engineered materials. Results indicate that grown material properties can be significantly modified through adjustments of easy-to-control cell culture inputs such as media hormone levels.

Materials and methods

Hormone-response verification experiment

Cells were isolated from young Zinnia leaves as described in *Beckwith et al.* [3]using methods inspired by Fukuda and Komamine [14]. Extracted Zinnia cells were cultured for 10 days in media at various levels (Table 1, Table 2) of two hormones (alpha-naphthaleneacetic acid {NAA} and benzylaminopurine {BAP}) after 48 h in low-hormone media (Ze-M). The selected hormone concentrations are intermediate and repeated levels (e.g., Ze-M, Ze-I) of a previously conducted factorial experiment[3]. Cultures were maintained in the dark throughout on a shaker operating at 80 rpm. Sample aliquots were intermittently taken from each of the treatment groups and imaged after incubating with a live cell stain (Fluorescein diacetate {FDA}, Sigma Aldrich) and a cell wall stain (Calcofluor White {CW}, Sigma Aldrich).

TABLE 1

Treatment group and corresponding hormone levels. Asterisks indicate repeated conditions tested in previous factorial experiment [3]; the remaining samples represent intermediate values not previously tested.

Treatment ID	NAA concentration (μl/L)	BAP concentration (μl/L)
*1 (Ze-M)	1	1
*2	500	1000
*3 (Ze-I)	1000	1000
4	250	250
5	250	1250
6	750	750
7	1250	250

TABLE 2

Recipe for preparing *Z. elegans* cell culture with X μl/L NAA concentration and Y μl/L BAP concentration corresponding to quantities in Table 1·

Product Name	Supplier	Quantity [per liter of medium]
N616 Nitsch Medium	Phytotech Laboratories	2.21 g
Sucrose	Sigma Aldrich	10 g
Mannitol	Sigma Aldrich	36.4 g
α-Naphthaleneacetic acid (NAA)	Sigma Aldrich	X*
6-Benzylaminopurine Solution (BAP)	Sigma Aldrich	Y*

* X μl of 1 mg ml^{-1} NAA Stock Solution, Y μl BAP Solution.

Fluorescence imaging and analysis

To image cultures, 20 μl FDA stock solution (at 2 mg ml^{-1} acetone) was added per ml of culture and incubated in the dark for 20 min. Next, 250 μl CW was added per ml of culture and incubated in dark for additional 5 min prior to imaging. A Zeiss LSM780 confocal microscope was set to excitation/emission wavelengths of 265 nm/440 nm (DAPI filter) for CW and 490 nm/526 nm for FDA imaging. For gel media incubation, times were extended to 45 min each. Image analysis was performed using Image-J. The thresholding tool was used to select the relevant cell areas. To ensure robustness of the analyzed data ranges, the images corresponding to the highest and lowest values for a single sample were analyzed a total of 3 times, with the repeated results averaged to yield a final value for the given image. Imaged cultures were quantified by four metrics: live fraction, lignification metric, enlargement metric, and elongation metric [3]:

- The *live fraction* is the ratio between the percentage of the micrograph occupied by cells marked with a viability probe (FDA), A_L, and the percentage of the micrograph occupied by all cells marked with a cell wall stain (CW), A_T, i.e.,

$$Live\ Fraction\ [\%] = 100\% * \frac{A_L}{A_T} \tag{1}$$

- The *lignification metric* is the ratio between C_L—the number of lignified cells in the micrograph exhibiting secondary cell wall patterning of tracheary elements (Fig. 1), and the corresponding A_T, i.e.,

$$Lignification\ Metric\ [\%^{-1}] = \frac{C_L}{A_T} \tag{2}$$

- The *enlargement metric* is the ratio between C_{En}—the number of cells in the micrograph with a maximum dimension greater than a certain threshold, and the corresponding A_T, i.e.,

$$Cell\ Enlargement\ Metric\left[\%^{-1}\right] = \frac{C_{En}}{A_T}; \tag{3}$$

the threshold value for cell enlargement, l_α, represents the maximum dimension of cultured cells at 48 h after cell isolation (l_α is approximately 84 μm for the Zinnia model used).

- The *elongation metric* is the ratio between C_{El}—the number of cells in the micrograph with a maximum dimension greater than a certain threshold, and the corresponding A_T, i.e.,

$$Cell\ Elongation\ Metric\left[\%^{-1}\right] = \frac{C_{El}}{A_T}; \tag{4}$$

the threshold value for cell elongation, l_β, represents the maximum dimension of cells grown in low-hormone media for 12 days that exhibit multi-directional enlargement without pronounced uniaxial elongation (l_β is about 119 μm for the Zinnia model used).

In analzying a sample at a given time point, all four metrics were obtained from the same set of micrographs.

Net-shape plant material production

Cells were isolated from young Zinnia leaves as described in *Beckwith et al.* [3]. After 48 h incubation in liquid medium, cells were concentrated for 3D printing. Gel media, with 4 g/L Gelzan postprint concentration, was autoclaved and then maintained at 60 °C in a water bath to prevent solidification prior to printing. To print, liquefied gel media and concentrated cell solution (prepared at four times the desired cell concentration for the final gel culture, e.g., a concentrated solution of 2×10^6 cells/ml was prepared to achieve a final gel culture concentration of 5×10^5 cells/ml) were combined 3:1 (v/v) and loaded into a 10 ml syringe equipped with an 18-gauge blunt-tipped needle. Approximately 4 ml (only enough for a single print) was loaded at once to reduce prolonged exposure of cultures to elevated temperatures. A Tissue Scribe bioprinter (3D Cultures, Philadelphia PA) extruded

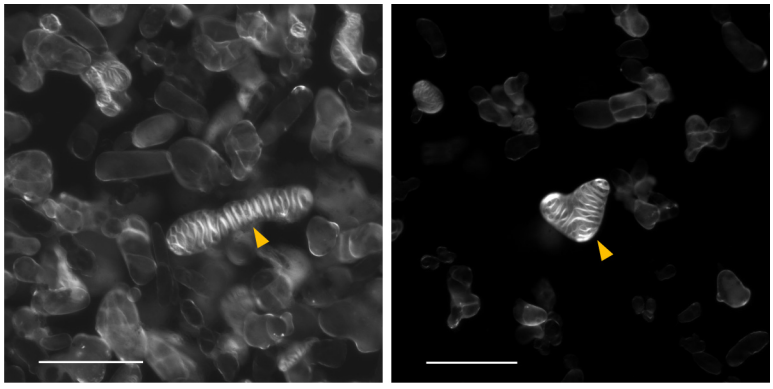

FIGURE 1

Differentiated cells exhibit unique secondary wall patterning visible in fluorescence micrographs. The secondary cell walls of plant cells differentiating into vascular cell types, exhibit patterned secondary wall thickening. Because of the elevated cellulose concentration in the thickened cell walls, vascular cell types fluoresce brightly in the presence of Calcofluor White compared to undifferentiated cells. Arrows indicate examples of tracheary elements. Scale bars represent 100 micrometers.

the gel solution into a petri dish while executing a G-code file with the geometry of the printed object and the associated printing parameters. During the printing process, the syringe temperature was maintained at 52 °C to prevent solidification of the gel within the syringe. After printing was completed, the cell-doped prints were sealed with parafilm and incubated in the dark at 22 °C for 3 months unless otherwise noted. After the first 3 days of incubation, 1 ml of liquid media matching the gel media formulation was introduced to the petri dish to ensure that the samples did not dehydrate too quickly. Then, every 7 to 9 days, the petri dishes were briefly opened to allow for gas exchange; if the sample was dry (supplementary liquid has been taken up), an additional 1 ml of liquid medium was added to the petri dish to wet the sample.

Plant material post-cultivation processing

At the end of the 3-month incubation period, samples were rinsed twice with deionized water by flooding the petri dish; the samples were then released from the petri dish by completely submerging the sample in deionized water and nudging gently along its edges with a flat utensil. Using filter paper, samples were carefully transferred to and sandwiched between two flat surfaces covered in Teflon sheets. Inverted petri dishes and covers were found to be useful for this purpose. Care was taken to not crush the samples. Small filter paper strips were placed in contact with edges of the wet samples to facilitate dehydration. Drying samples and associated fixtures were stored in a desiccator until dehydration was complete (usually 3 to 4 days).

Physical characterization of plant materials

Physical characterization of the samples included measuring their mass and volume. Length and width of rectangular, 3D-printed samples were measured using calipers. Length was measured at three locations along the sample width and the measurements were averaged; similarly, width was measured at three locations along the sample length and the measurements were averaged. Likewise, sample thickness was measured using a benchtop micrometer; the sample thickness was measured at three locations along the sample length and the measurements were averaged. The mean length, width, and thickness values were taken to be the absolute length, width, and thickness of the sample for downstream calculations of sample volume. Sample density was obtained by dividing sample mass, determined with a mass balance, by the calculated sample volume. For the purposes of the enclosed analyses, where the priority is understanding trends rather than absolute mechanical properties, the density measurement of a given sample was assumed to be exact (i.e., with an error of zero) for ease of standard deviation reporting. For a particular treatment group, the masses or densities are presented as averaged values across measured samples with sample standard deviations reflecting the variance between the assumed "exact" sample-specific values.

Autofluorescence imaging of hydrated gel cultures

Natural autofluorescence of cell wall molecules allows for non-destructive visualization of cellular components. For lignin visualization, samples were imaged on a Zeiss LSM 780 fluorescence microscope at two excitation/emission pairs (355/488 nm and 455/535 nm, respectively). Taken individually, these excitation wavelengths can produce fluorescence in a range of natural fluorophores. Overlaying signals from both excitation/emission pairs allows for lignin visualization as lignin fluoresces at both settings [12].

Cross-sectional imaging of dehydrated plant samples with fluorescent probes

Samples were embedded in paraffin wax and then sliced into thin sections using a handheld microtome (Carolina Biological Supply Company). Cross-sectional slices were transferred to a microscope slide and wetted with 10 μl of CW diluted in media (1:3 v/v) for visualization of plant cell walls[5,17]. Samples were imaged on a Zeiss LSM 700 fluorescence microscope at 265/440 nm (DAPI setting). When lignin visualization was also desired, 10 μl of an Acriflavine working solution prepared at 0.00624 mg/ml water was also added to the sample section. The Acriflavine stain was imaged at 488/530 nm to visualize lignin[21,9]. Samples were imaged promptly. Samples were imaged repeatedly at a narrow rangeof focal planes. Between 1 and 8 images per sample were stacked using Adobe photoshop 'Auto-blend' feature to produce composite images of sliced surfaces with improved clarity.

Mechanical characterization of plant materials

Rectangular, bioprinted samples were prepared, cultivated, and dehydrated for mechanical characterization via dynamic mechanical analysis (DMA). Time sweeps of applied, oscillating strains were imparted using a TA instruments Discovery Hybrid Rheometer-2 with the Film Tension Clamp fixture to ascertain elastic and viscous moduli values for dehydrated samples. Tests were performed at 0.01%, below the determined critical strain, at a fixed frequency (0.1 Hz), and at constant temperature (20 °C). Force, reported as stress, was measured in response to the applied strain and used by the equipment's software to automatically calculate the storage modulus (G′) and loss modulus (G″) of the tested materials. Over the course of a DMA time sweep, samples were strained and relaxed multiple times, allowing for numerous replicate measurements to be taken on the same sample. With time, measurements stabilized. Sample-specific average measurements for G′, G″, and tan(δ) were obtained by averaging the values across the stable region; these individual sample averages were subsequently averaged across multiple samples, to obtain reported average values and standard deviations. Samples for which DMA data are compared directly were generated on the same dates with the same cellular feedstock and grown for the same duration prior to dehydration. The media composition of the samples varied as indicated in the results.

Statistical inference

When comparing two sets of sample data, P-values were determined using Matlab's t-test function. Unless otherwise stated, error bars on graphs represent one standard deviation above and below the mean.

Results and discussion

For cultured materials, understanding the relationship between cellular characteristics and material properties requires investigation at multiple length scales. First, cell-scale development is investigated, as comparative data on cell development in response to hormonal variation clarifies the relationship between certain developmental pathways and the impact of biological variability on culture outcomes. Then, scaling up, bioprinting and casting techniques are used to define the limits of the culture environment, defining the structures of the cultured materials by constraining and directing regions of cell growth; using these methods, materials are cultivated in forms and at scales not readily available in nature. Finally, knowledge of cellular tunability and form control are used to generate material samples that are characterized to reveal their physical properties, mechanical attributes, and microstructural characteristics. The suite of results provides insights on the impact of controllable adjustments to media formulation on the ultimate cultivated material properties.

Control of cellular-level properties

Media formulation can impact cell fate and, in conjunction, cell wall compositions (e.g., proportion of pectins, proteins, cellulose, lignin) and physical attributes (e.g., shape, thickness, stiff-

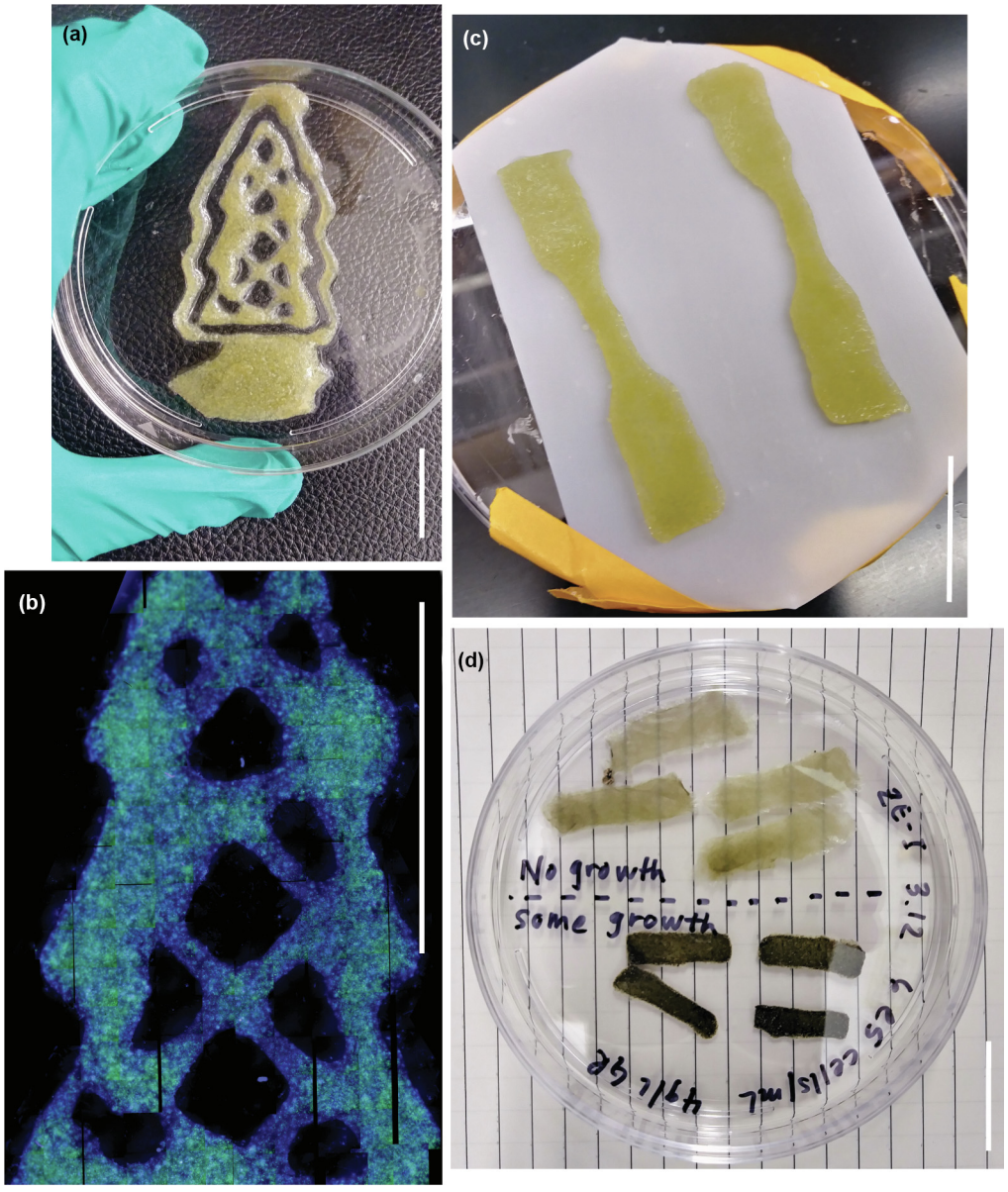

FIGURE 2

Grown materials can be produced in forms not naturally available. Selected examples of bioprinted, cultivated plant materials: (a) printed tree-shaped culture in 10 cm-diameter petri dish, standard lighting at 3-months old, (b) stitched, two-channel autofluorescence micrograph of tree-shaped print in which the coincidence of green and blue channels indicates likely presence of lignin, (c) dog-bone structures after transfer to a drying plate (an inverted 10 cm-diameter petri dish), (d) bioprinted, cultured, and dehydrated samples without growth (top samples) and with growth (dark green, bottom samples). All scale bars represent 2.5 cm.

ness). In nature, variations to these chemical and physical cell wall traits lead to differences in material-level properties. As such, tuning the cellular-level characteristics in lab-grown materials is also expected to be critical for controlling emergent material attributes.

In this work, comparing cell development across culture conditions and across unique pools of biological samples helps clarify the relationships between certain cellular-level characteristics (e.g., lignification and elongation metrics). Experiments to assess cellular response to varied media formulations were performed on freshly initiated cultures and compared against published factorial experiment data obtained six months prior[3]. Cultures were maintained at either previously tested hormone levels or at untested intermediate levels, still within the limits defined in the original design of experiments (Table 1). Cell growth characteristics were then quantified using four metrics: live fraction, lignification metric, enlargement metric, and elongation metric. The results affirm the repeatability of previously reported development trends, point to culture attributes impacting the magnitudes of cellular response to environmental cues, and help to identify relationships between different development pathways. This knowledge could allow future efforts to strategize the sequential application of developmental cues to achieve the right magnitude and combination of cellular traits and accompanying material-scale properties.

Repeatability of cellular development trends

Cellular behavior, as quantified by the four metrics, trended with design of experiment (DOE) data previously published[3], indicating repeatability in response to hormonal variations across biological samples.

For live fraction, measurements corresponded well with reported values for cultures of the same age, particularly as cultures matured. For example, despite differences in live fraction starting values, low-hormone cultures tended to increase to levels nearing 80% by the twelfth day in culture for this data and data reported by Beckwith et al. (Fig. S.1). For repeated experimental conditions (i.e., media *1, 2,* and *3*), daily live fraction is plotted for both the original and verification experiments (Fig. S.1) and correlations are evident. For new verification test

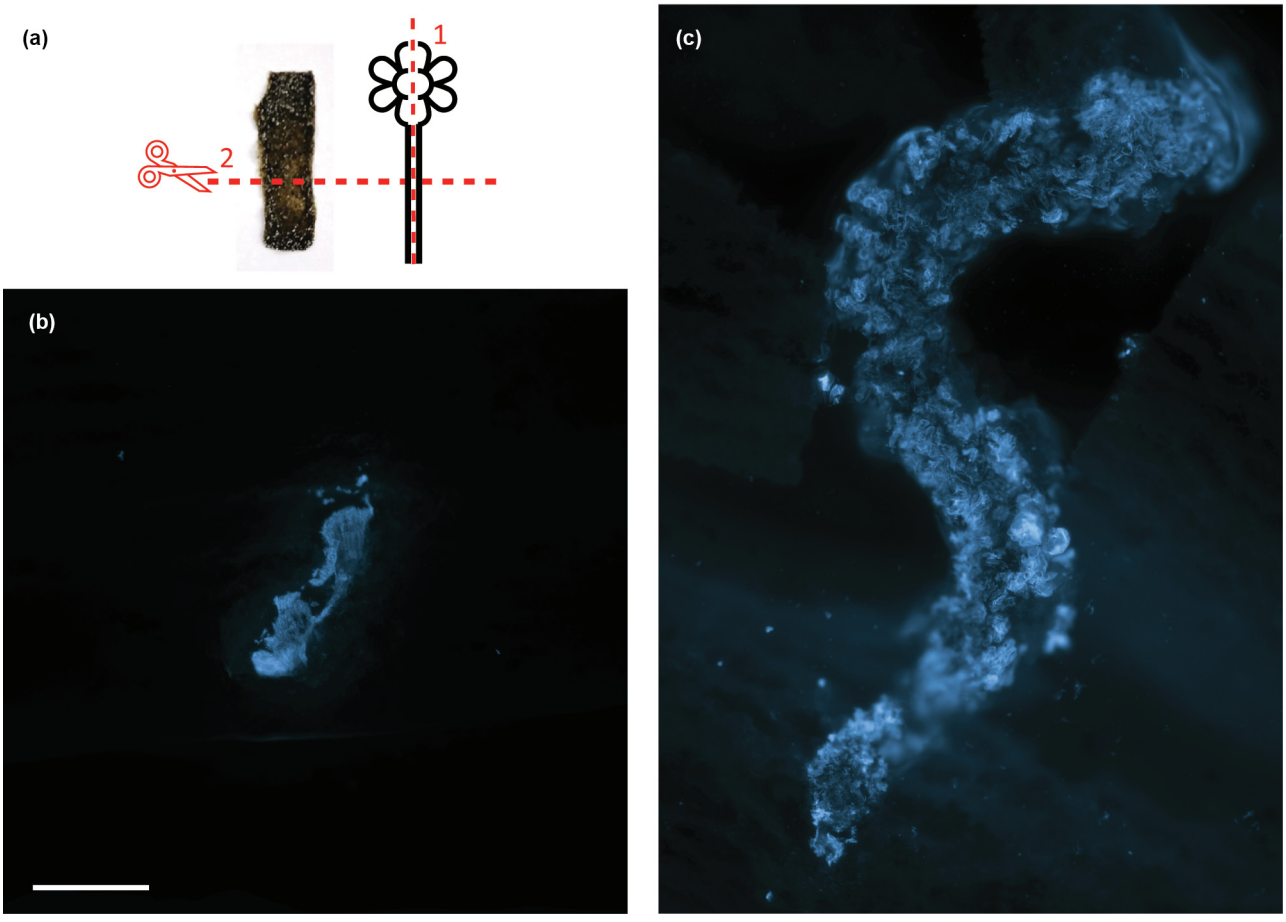

FIGURE 3

Grown materials can be produced at scales larger than naturally achievable. (a) Materials were sectioned as shown. Stem samples were halved lengthwise (cut 1) and dried before fixing in wax and sectioning with a microtome along the indicated cut 2. Dehydrated cultured samples were fixed in wax and sections and sectioned as indicated in cut 2 and stained with CW to illuminate plant cell wall material. (b) A cross-section of a halved and dried Zinnia stem–which is small in scale compared to the sizes accessible by the proposed direct-material growth method for the same growth time. (c) A cross-section of a grown material sample sliced along the shortest dimension. Two images are stitched together to visualize the whole extent of the sample. The sample curvature is a result of the fixing, slicing, positioning, and staining processes. Both samples are pictured at the same magnitude. Scale bar equals 500 micrometers.

conditions (i.e., intermediate hormone conditions *4, 5, 6,* and *7*), daily live fraction is compared against predicted values obtained by linearly interpolating the midpoint values from original DOE data (Fig. S.2). Again, this data corresponded well with the predicted values developed based on prior data[3]. The deviation from predicted values seen for media 5 may be result from non-linearity of cellular response, and thus prediction inaccuracy, in this region where change in original DOE live fraction is pronounced across the sector[3].

Similarly, for the lignification metric, development trends remained consistent with reported values (i.e., media 2 and 3 exhibiting highest levels of lignification for the tested media selections, and media *1,* the lowest). Cumulative and daily lignification metrics peaked in the range of 500–1000 μl/L NAA and 500–1000 μl/L BAP and these formulations (media 2 and 3) with media formulations *6* and *7* span the region of maximal differentiation seen previously. Additionally, the inversion between lignification and live fraction metrics continues to be evident—even across unique Zinnia samples (Fig. S.3). Viability declined over time in cultures undergoing high rates of differentiation into tracheary elements.

As with the other metrics, cellular enlargement and elongation presented trends across media types consistent with original data (Fig. S.4). As in experiments by Beckwith *et al.*, enlargement metric was highest for low-hormone media formulations[3]. Interestingly, elongation tended to be pronounced in samples with lower levels of tracheary element differentiation.

Insights from shifts in magnitude of culture response to environmental conditions

Despite repeatability of trends seen for all four of the metrics, magnitudes of lignification, enlargement, and elongation metrics varied between the new data and previously reported values[3], indicating that other factors play a role in determining the responsiveness of cultures to environmental cues. Comparisons in the absolute values between new and original data highlight other key considerations in predicting culture outcomes.

In the new data, the magnitude of cumulative lignification measurements was elevated compared to the previously reported data. This shift in absolute value could be attributable to the increased starting live fraction seen in the new data (i.e., there are more viable cells capable of differentiating, and therefore, a higher effective cell density, which has been shown to improve differentiation rates), and to natural biological variation of Zinnia plant sources.

Meanwhile, net increases in enlargement and elongation metrics tended to be reduced in the new data compared to prior results (Fig. S.4). Reduced enlargement or elongation may in part be a secondary result of high differentiation rates (i.e., quantified by lignification metric). When induced to differentiate into tracheary elements, responsive cells commit rapidly to the developmental pathway and exhibit secondary cell wall deposition and the cessation of further growth within a matter of days[27]. On the other hand, elongation tends to become evident in later stage cultures. Thus, high differentiation rates would lead to a smaller pool of remaining cells with the potential for elongation. An in-depth assessment of the relationships between differentiation and morphological developments is warranted and would improve tunability of grown materials. For example, if early differentiation limits cell expansion, the delay of differentiation into vascular cell types until after the cells have enlarged may be necessary to achieve both enlarged and differentiated cells in grown materials. Interactions between these and other developmental outcomes will need to be uncovered and then considered in the design of material cultivation processes.

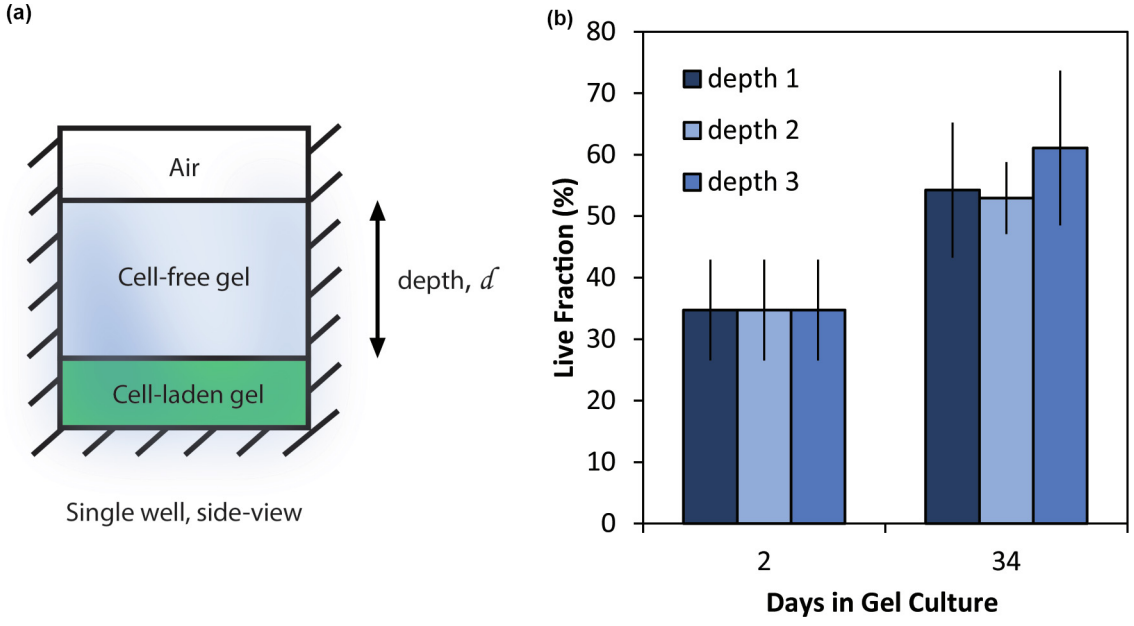

FIGURE 4

For cell cultures grown under gel depths up to 8.7 mm thick, cell survival was not impacted. (a) Cell-free gel media was deposited and gelled atop a cell-laden gel media mixture 2.5 mm thick. (b) Cells were cultured for 32 days beneath cell-free gel layers of various depths. Gel depth, *d*, was set to 2.5, 5, and 8.7 mm for depths 1, 2, and 3, respectively. Gel depth did not impact cell viability within the tested range (on day 34, P = 0.80, 0.18, 0.34 for sample-to-sample comparisons of depths 1 – 2, depths 2 – 3, and depths 1 – 3, respectively).

In summary, high-level trends in hormone-responsive development are consistent across biological samples. However, magnitude of response can be influenced by additional culture attributes. The presented data indicates that cell density and biological potency are potential "sensitizers" in the process of hormone-induced differentiation. The modulation of these culture characteristics seemingly alters cellular receptiveness to differentiation under the right hormonal conditions. Also notable, high rates of differentiation corresponded to reduced culture potential for further cellular enlargement and elongation. Understanding the relationships between culture inputs and developmental outcomes, as well as the relationships between pathways leading to key growth characteristics, will improve control of grown material attributes.

Material form and scale

In addition to cell-scale attributes, macroscopic features of the resulting materials can be controlled by shaping or constraining the physical limits of the growth environment. Hydrogel scaffolding is useful for stabilizing culture environments and suspending dispersed plant cells in both contained and freestanding arrangements[30,31,23,28,13]. Furthermore, scaffold-guided growth enables the production of materials both in forms and at scales that are not naturally occurring.

Bioprinting and casting techniques were used to deposit cell-laden scaffolds in the desired forms. Over the course of this work, various structures were seeded and cultivated to generate plant materials in pre-determined forms (Fig. 2). A primary advantage of using bioprinting is the technology's capacity to create structurally intricate growth environments for the growing cells, facilitating the production of plant materials in complex, customizable forms. Casting or molding techniques can often accomplish the same aims, but also offer the advantage of being amenable to high-throughput manufacturing of identical objects. An exact process flow should be selected on a case-by-case basis. This work aims to illustrate that the dispersed-gel culture format is well-suited to manipulation by either of these manufacturing techniques. Ultimately, net-shape manufacturing of plant materials during growth of plant materials has the potential to reduce waste and processing associated with standard practice.

Despite constraints in print size due to the limitations of available equipment, materials were cultivated at scales larger than comparable materials present in a similarly aged plant. For exam-

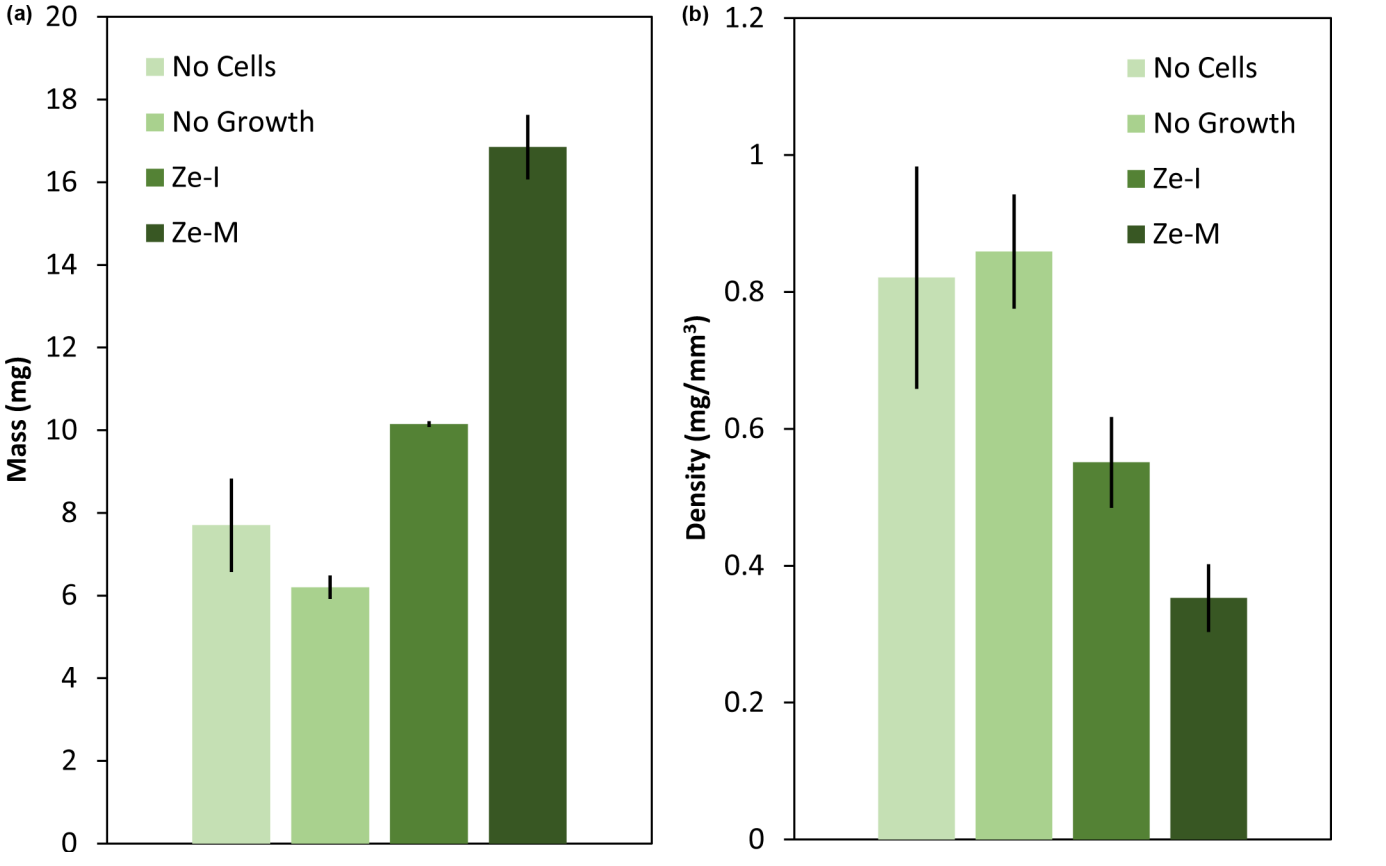

FIGURE 5

Mass (a) and density (b) of samples cultivated in different media. Samples grown in Ze-M medium experience the greatest increase in mass, and the greatest reduction in density. Both Ze-I and Ze-M samples exhibit notable changes in mass and density compared to cell-free and growth-free controls. Comparisons of Ze-M sample mass/density to No Growth and No Cells samples yielded P-values of 0.017/0.060, 0.003/0.018, respectively. Comparisons of Ze-I sample mass/density to No Growth and No Cells samples yielded P-values of 0.003/0.055, 0.092/0.161, respectively. Samples were seeded at an initial density of 6×10^5 cells/ml and cultivated for 3 months.

ple, Fig. 3 depicts a cross-section of a grown material sample next to a cross-section of a Zinnia stem, halved and dried. These demonstrations indicate the potential of culture techniques to directly produce materials in forms and scales more useful for downstream applications.

Because required nutrients and hormones are incorporated within the scaffold itself, this fully contained setup requires little intervention after deposition. The scaffold can sustain growth through differentiation and to confluency without the support of active perfusion systems. Cultures can survive and continue to grow for months after printing.

For the purposes of these early investigations into net-shape plant material production, grown structures were kept to planar, relatively thin configurations. Translation to larger scales will require cell survival in thicker structures. To investigate survival at greater culture dimensions, cell cultures were plated at various gel depths (distances from the gel-air interface) in 24-well plates (Fig. 4a) and allowed to grow for 32 days. For depths evaluated (i.e., 2.5, 5, 8.7 mm atop a 2.5 mm – thick cell culture), there was no apparent impact on live fraction after 32 days in culture gel culture (Fig. 4b) ($P > 0.18$ for all sample-to-sample comparisons on day 34). All samples exhibited an increase in live fraction from initial seeding to final evaluation. These results indicate that growth of thicker structures is possible, the potential scalability of these structures is in part due to the permeability of the hydrogel matrix which makes up the local cellular environment and the slow growth of cells relative to animal or bacterial cell systems.

Physical, mechanical, and microstructural characterization of lab-grown plant materials

While great progress has been made in the investigation of relationships between processing conditions in 3D cultures with microstructural properties in tissue engineered constructs[16], these advances have largely been limited to research with animal cells. With the newness of selective-growth of plant materials in 3D culture environments, this work presents the first characterizations of these products and provides insights into the relationship between plant cell development in culture and material properties in a final, dehydrated state. To assess characteristics of the produced materials and benchmark progress for future comparisons, selected physical and mechanical properties, and the microstructure of the cultivated samples were investigated. Results indicate that both macro-level and micro-level properties are significantly impacted by selected media formulation. Samples grown in two culture formulations, Ze-M and Ze-I (Table 1 and Table 2), were evaluated. Ze-M media is intended to support growth and proliferation without differentiation of cells, whereas Ze-I media is formulated to induce cells to form vascular cell types with thickened and lignified secondary cell walls. Natural zinnia samples were prepared from the stem of the Zinnia plant which was harvested at the same age as cultured samples. While stem samples were useful in preparing cross-sections for microstructure visualizations, the samples were too small and lightweight to be accurately measured using the physical and mechanical measurement techniques available for this work—evidencing how lab-grown tissue techniques enable faster growth of materials in useful forms.

Physical properties

In addition to influencing single-cell development, differences in media formulation can also impact cellular proliferation (i.e., final cell density, final plant mass accumulation). In both Ze-M and Ze-I samples, increases in plant mass led to detectable changes in final sample mass relative to control samples printed without cells and samples with cells that experienced no growth after printing. Materials grown in a low-hormone, maintenance media (Ze-M) base exhibited the largest gains in accumulated plant mass (Fig. 5a), followed by cultures grown in high-hormone, induction media (Ze-I). In Ze-I media, cell populations are induced to differentiate into tracheary elements; the rapid transformation and subsequent programmed cell death leaves behind a smaller population of cells with the capacity for continued growth. These Ze-I samples thus tend to amass a smaller quantity of plant material compared to samples grown in Ze-M maintenance media. Interestingly, despite the greater plant mass accumulation in Ze-M samples, density is reduced compared to both Ze-I samples and samples without growth (Fig. 5b).

Looking at the mass and volume changes as a percentage relative to the cell-free control, both Ze-M and Ze-I samples again demonstrate notable increases in both mass and volume relative to cell-free and growth-free controls (Fig. 6). However, Ze-M samples exhibit proportionately larger changes in volume compared to mass, with a volume increase nearly four times larger than

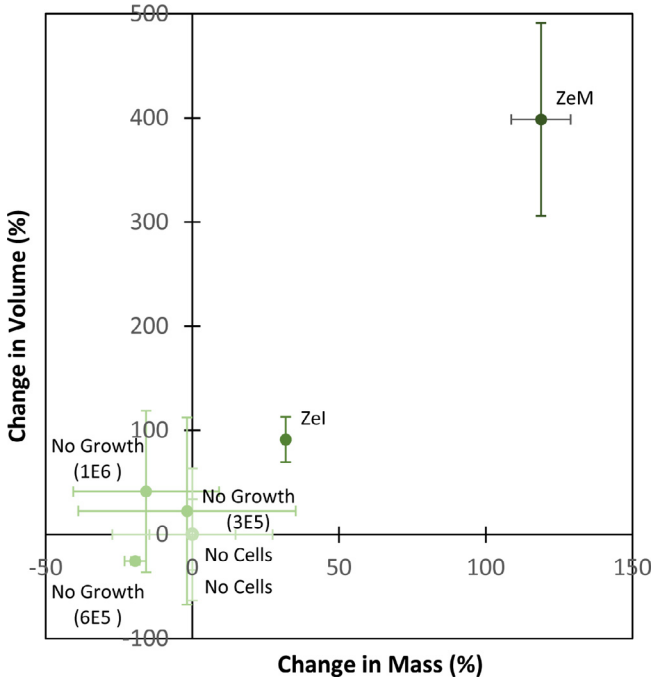

FIGURE 6

Percent increases in mass and volume of samples grown in various media compared to cell-free and growth-free control. Sample cultivated in Ze-M exhibit a volume increase nearly four times larger than mass increase. Meanwhile, samples in Ze-I exhibit a volume increase not quite two times larger than mass increase. Grown samples were seeded at an initial density of 6×10^5 cells/ml and cultivated for 3 months, measurements were also made for growth-free samples prepared at various cell densities: 1×10^6, 6×10^5, 3×10^5 cells/ml.

mass increase. By contrast, Ze-I samples exhibit a volume increase not quite two times larger than mass increase. These unbalanced ratios between mass and volume gains suggest underlying differences in the material microstructure.

Mechanical properties

For cellular materials cultivated under various growth conditions, strain-controlled dynamic mechanical analysis (DMA) was performed to assess mechanical properties. DMA enables the non-destructive assessment of mechanical properties through the application of a small-amplitude, oscillating strain and evaluation of sample response. Unlike uniaxial testing, in which samples often undergo extensional strain beyond the Hookean regime and to failure, DMA can be performed entirely within the Hookean or linear viscoelastic regimes[22]. When performing DMA, a test sample is positioned between two fixtures: one stationary, and another that imposes a time-dependent, sinusoidal strain. The resulting time-dependent stress is simultaneously monitored by quantifying the torque generated on the stationary fixture[29]. The relationship between applied strain and simultaneously recorded stress data provides insights into the mechanical properties of the tested sample. The phase shift between the two curves, is used to determine the storage modulus (ratio of elastic or in-phase stress to strain) and loss modulus (ratio of viscous or out-of-phase stress component to strain). Effectively, the storage modulus represents the material's elastic behavior or stiffness whereas loss modulus relates to the material's capacity to dissipate energy. It should be noted that the storage modulus and Young's modulus are conceptually related but are not the same[24]. When the storage modulus exceeds the loss modulus, the material displays predominantly elastic behavior. For perfectly elastic materials, with stress and strain linearly related, the stress strain curves are in phase ($\delta = 0$) as the materials immediately return to their original form upon removal of applied strain. Purely viscous materials exhibit a phase shift of 90° ($\delta = \pi/2$).

Rectangular strip samples were prepared in either Ze-M or Ze-I medium (Table 1 and Table 2) by means of bioprinting, incubation, and subsequent dehydration. When analyzed by DMA, varying media hormone concentrations of grown samples was found to generate significant differences in the resulting storage modulus of cultivated samples. The storage modulus values of differentiated Ze-I samples were higher than measured storage modulus values for undifferentiated Ze-M samples ($P = 0.033$) (Table 3). Potential reasons for this difference in mechanical properties include: different levels of cellular entanglement, differences in plant matter composition (e.g., cell wall composition and structure), and differences in plant/gel fraction resulting from differences in mass accumulation between treatment groups. Ultimately, improved control of growth across cultivation conditions will be needed to fully untangle the contributions of these parameters towards final material characteristics. A measurement of dehydrated gel samples without plant materials is included in Table 3 for reference. Storage modulus for gel is notably higher than grown plant samples; this is likely due to several factors including increased sample density (as a result of reduced porosity and compositional differences) and natural stiffness of the single-phase gel material being higher than the stiffness of cultivated plant matter. Cell-free, gel materials are a useful reference for calibration, but are perhaps not useful benchmarks of progress towards *in vitro* plant material production. To contextualize the results presented in Table 3, available data on properties of natural plant materials are helpful references. Reported storage modulus values for woods have been reported in the range of 300–1200 MPa[19,1], although exact values can vary with testing apparatus, setup, and sample grain orientation. In any case, DMA measurements for lab-grown samples appear to correspond well to the storage modulus measurements for natural tissues. While the shifts to storage modulus that result from tuning culture environment cannot yet be precisely attributed to a specific cause, the presented DMA results provide a compelling indication of the tunability of cultured materials by simple modifications to controllable system inputs.

TABLE 3

DMA results for cultures grown in Ze-M maintenance medium and Ze-I induction medium; n = 3–4 samples per treatment group. For a small angle, $\tan(\delta) = \delta$.

Medium Type	Storage Modulus (MPa)	Loss Modulus (MPa)	tan(*δ*)
Ze-M	138.3 ± 57.4	8.365 ± 4.47	0.065 ± 0.031
Ze-I	404.7 ± 146.9	16.0 ± 11.1	0.037 ± 0.014
Gel, No Cells	1451.0 ± 645.7	164.88 ± 127.6	0.100 ± 0.002

Microstructure

Beyond cell wall composition, cellular form can also impact the dehydrated material properties by influencing the material microstructure. Microstructural characteristics of cultivated materials were assessed by embedding samples in paraffin wax, sectioning the sample with a handheld microtome, and staining the sample section with fluorescent cell wall markers. In the resulting fluorescent micrographs, structural differences are evident between samples which did or did not experience growth, as well as between materials grown in different media formulations (Figs. 7, 8).

The difference in microstructure across samples is stark. In samples without growth, cells are discrete, flattened structures with no interconnectedness. By contrast, grown samples are notably thicker and contain a higher proportion of visibly fluorescing plant wall material. Ze-M samples yield an open microstructure, with rounded cells which retain their shape upon dehydration. This aligns with the substantial volume increases seen in Ze-M materials relative to controls. In Ze-M samples, opportunities for interconnectedness or entanglement are reduced by the nature of the predominantly round cell shape. On the other hand, Ze-I samples exhibit a tightly packed network of plant material with a variety of cell configurations which could lead to increased interlocking of the plant material phase.

Cross-sectioned samples were also imaged using a dual-stain approach to allow for visualization of both cell wall material and lignin (i.e., using CW and Acriflavine, respectively) (Fig. 9). In Ze-M samples, a lack of localized Acriflavine fluorescence indicates low levels of lignification[21], as is expected from the maintenance media formulation. On the other hand, for Ze-I samples

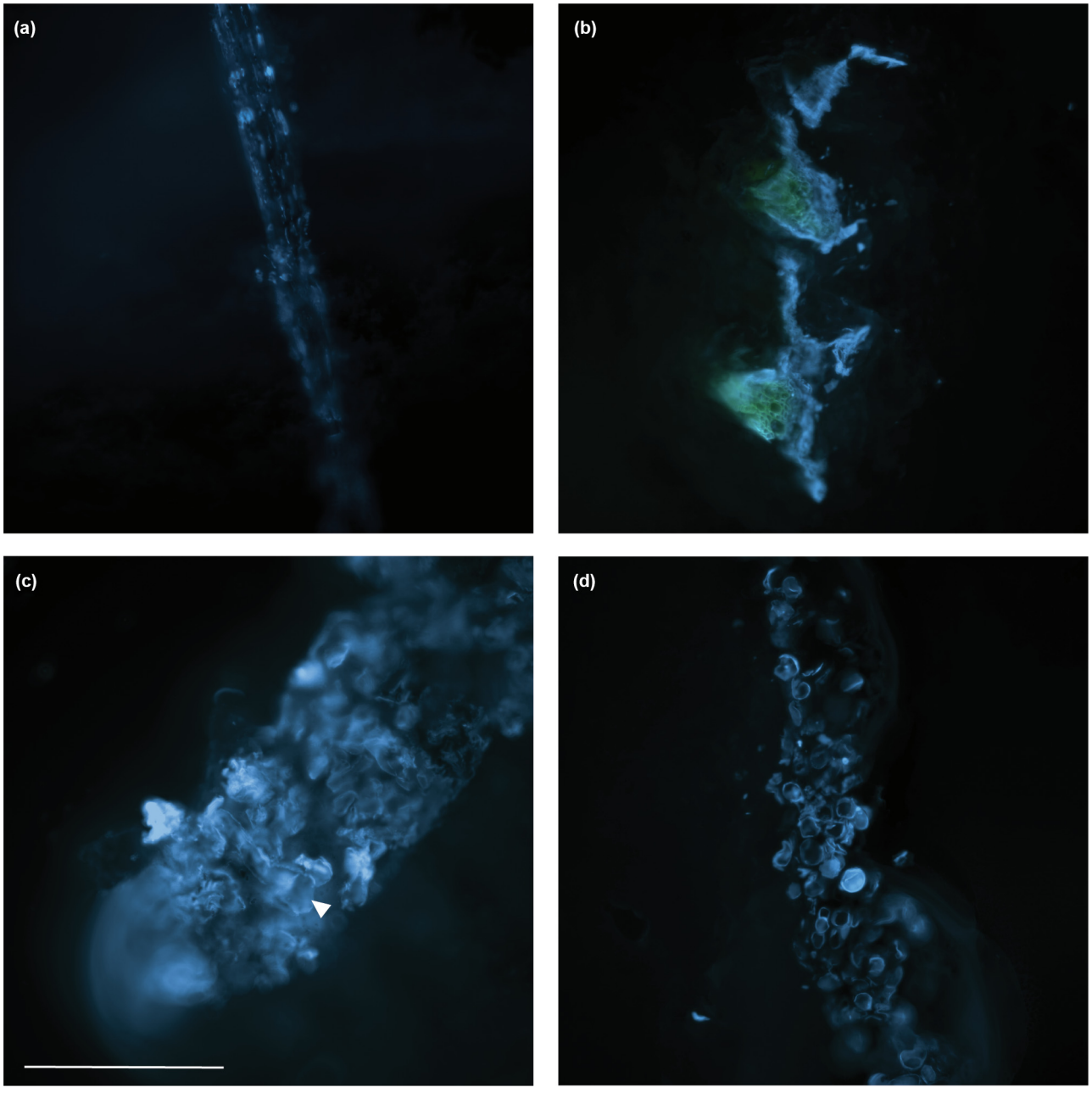

FIGURE 7

10x cross-sectional images of various prepared samples and Zinnia stem using CW stain to indicate cell walls. (a) Growth-free samples exhibit limited and discrete fluorescence where cells have flattened in the dehydration process without convalescing. (b) A halved and dried Zinnia stem, with vascular tissue indicated in green using Acriflavine stain, is delicate, non-homogeneous and small in scale compared to printed samples. (c) Ze-I sample shows dense cell growth. Some elongated cells are visible and cells show good apparent interaction. An arrow indicates an elongated cellular structure which stretches from the arrow to the opposite side of the sample. (d) Ze-M shows open material structure with thick-walled, rounded cells. The cell-to-cell interaction appears to be limited, although some local connectivity may be present. All samples are pictured at the same magnitude. Scale bar equals 500 micrometers.

grown in induction medium, fluorescent regions of lignification are interspersed throughout the sample. By comparison, the stem shown comprises multiple tissue types, but the vascular tissue of interest is visible when lignin is fluorescently labeled as well. Naturally the stem presents denser, more structured growth. However, xylem tissue is localized to small regions of the stem whereas un-patterned materials with greater consistency across sample locations are achievable using culture methods.

Summary of findings

Variations in absolute results between experimental iterations investigating cell response to hormone levels highlight relationships between various developmental pathways. High differentiation rates lead to reduced viability; therefore, cultures induced to differentiate early-on see reduced plant matter accumulation in long-term cultures compared to undifferentiated cultures. High rates of differentiation also corresponded with reduced

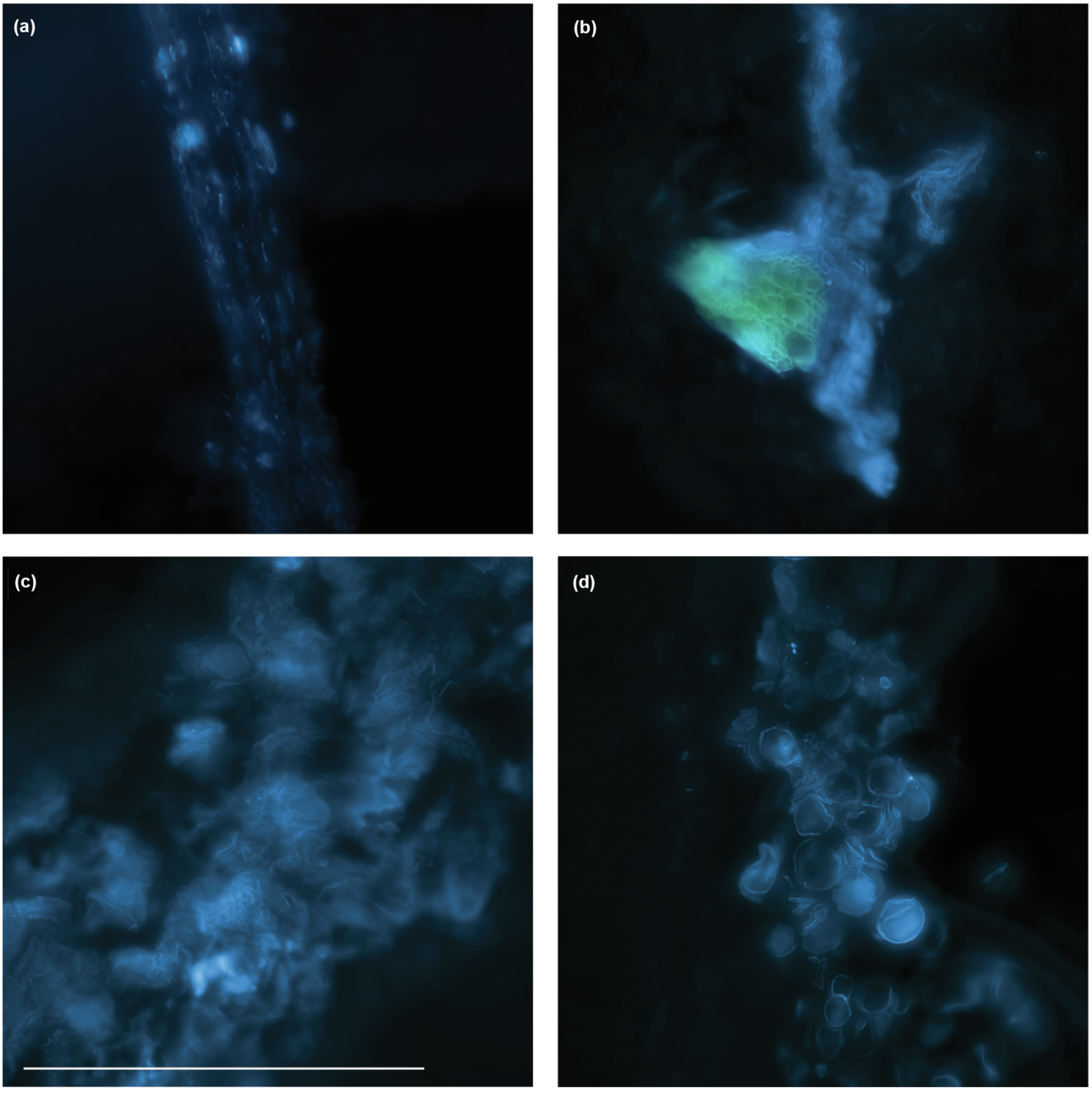

FIGURE 8

20x cross-sectional images of various prepared samples and Zinnia stem. Blue coloration indicates cell walls made visible using CW stain. (a) Growth-free samples exhibit limited and discrete fluorescence where cells have flattened in the dehydration process without convalescing. (b) A Zinnia stem, halved with vascular tissue indicated in green–allowed by staining with Acriflavine, shows tightly-packed cells with lumen of various sizes. (c) Ze-I sample shows dense cell growth and what appear to be frayed secondary cell wall structures of TE's. These structures were likely disturbed during the sectioning process. (d) Ze-M shows open material structure with rounded cells which are well-preserved despite the dehydration process. The cell-to-cell interaction appears to be limited in the Ze-M sample, although some local connectivity may be present. All samples are pictured at the same magnitude. Scale bar equals 500 micrometers.

enlargement and elongation in cultures, perhaps because of differences in relative timescales of these developmental processes. Otherwise, previously reported trends are repeatable, although the magnitude of response may be modulated by sample biology.

Knowledge of relationships between development characteristics may help to define improved development sequences in future materials production (e.g., developing a system made up of both elongated and differentiated cells may first need to direct elongation followed by later-stage differentiation). Sequential development could improve the final likeness of the material to natural plant tissues and serve to increase the range of achievable macroscopic properties.

New forms and scales are available in cultured materials compared to natural plant tissues evaluated on the same timescale. The limits of gel culture thickness allowing for long-term cell survival have not yet been identified. Results indicate that cells can survive at more than 8.7 mm distance from the gel surface for at least 32 days.

RESEARCH: Original Research

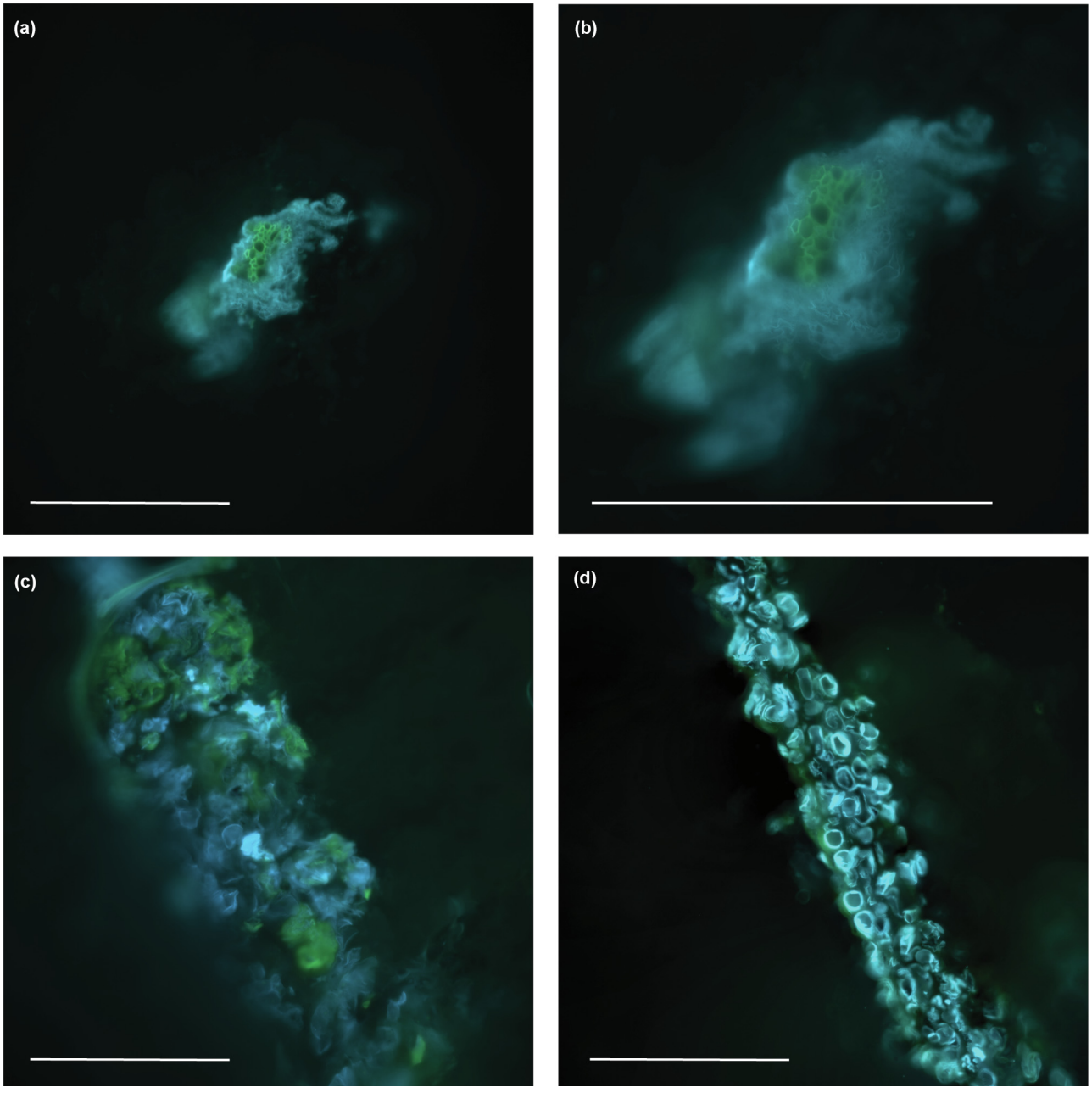

FIGURE 9

Dual-stained sample cross-sections allow for cell wall and lignin visualization. Light blue coloration indicates cell walls, green coloration indicates lignin as stained using Acriflavine. In dried Zinnia stems, imaged at 10x (a) and 20x (b), lignin is localized to a small bundle of vascular tissue. In Ze-I samples (c) Acriflavine fluorescence is dispersed throughout the sample cross-section. In Ze-M samples, there are no obvious regions of specific Acriflavine fluorescence supporting the expected lack of lignified cells. All scale bars represent 500 micrometers.

Variations to culture conditions, in this case modification of hormone levels, impacted physical properties, microstructure, and mechanical properties of the resulting materials in a significant degree. Variations to culture conditions also impacted plant matter composition, enabling the creation of chemically variable materials. Thus, with simple modifications to culture inputs, materials can be tuned to express a range of characteristics, demonstrating control of materials growth on the cellular and macroscopic scales.

Conclusion

Towards the pursuit of lab-grown plant materials, this work begins to elucidate the relationship between cellular-level characteristics (i.e., micro-scale) and emergent material properties (i.e., macro-scale). Characterization of resulting physical properties, mechanical attributes, and microstructural characteristics indicate that alterations to culture media formulation, and thus cell-level development, significantly impact material traits. Additionally, culture forms are shown to be controllable by targeted

hydrogel scaffold deposition using bioprinting techniques—demonstrating various forms and scales of grown materials that are not available using traditional agricultural methods. Experimental results also show that bioprinted samples can be significantly thicker without affecting cell growth. Further work on precision control of culture growth will help to further clarify the relationship between specific cellular properties and the resulting effects on material characteristics. Given the newness of these pursuits in net-shape, tunable, lab-grown plant materials, these results illustrate the promise of selective plant material production. Although these investigations are carried out on a model system, *Zinnia elegans*, rather than a true wood-forming plant, the developed methods and tools provide a framework for the translation of these concepts to other plant species. In a woody species, one could similarly employ a nutrient-rich, structured gel culture environment to facilitate cell growth and proliferation and then manipulate environmental factors, such as relevant hormones or chemical cues, to encourage morphological development and differentiation into vascular cell types. The resulting materials would exhibit wood-like attributes and could likewise be grown in a tree-free manner in defined shapes and with tunable properties.

Future work

Efforts towards the production of *in vitro* tissue-like plant materials are still in the early stages. The field would benefit from improved understanding of and control over cellular development, improvements to synchrony and uniformity of cellular development, and a deeper exploration of the relationship between cellular-level characteristics and resulting material properties. To better monitor and track culture development, additional measurement techniques should be developed to track cell proliferation through time. While culture growth can be assessed using image-based techniques like those utilized in this work, image-based confluency assessments are likely to become less useful for 3D systems at high culture densities. Spectrophotometric techniques may be useful in tracking gross culture densification. Other external (e.g., electrical and chemical gradients [15], scaffold properties, applied forces, etc.) and genetic factors on cell development should be explored to better our understanding and capacity to direct cell growth in gel cultures. A number of external and genetic factors are known to influence development in other *in vitro* and *in vivo* systems and may prove to modulate plant cell culture development as well [8,20]. Implementation of genetic tools could enable improved rates and timing of differentiation to improve homogeneity of produced materials. Meanwhile, a deeper analysis of the relationships between cell wall properties, cell-matrix interactions, and the results on emergent material properties are needed to be able to better predict material outcomes based on expected culture developments. With further maturation of presented techniques, entirely new plant-based materials could be possible—with spatially controlled microstructures and properties or multi-species materials derived from a monolithically grown culture.

Upon translating techniques to new species, additional research will be required to identify species-specific growth and development requirements. With further development, the proposed material growth could overcome unavoidable challenges in traditional cultivation. With land-free, sunlight-free growth, materials could be produced locally, anywhere in the world, regardless of climate. With on-site production in near-final form, the need for energy-intensive harvest, hauling, and processing is reduced. Finally, because of the homogeneity of the materials, yields of useful plant materials as a proportion of total plant material are potentially much higher than allowable in nature. As the process for selective cultivation of plant materials matures, a thorough analysis will be needed to determine the conditions under which such a process can be economically and environmentally advantageous over traditional agricultural methods.

CRediT authorship contribution statement

Ashley L. Beckwith: Conceptualization, Methodology, Investigation, Project administration, Formal analysis, Visualization, Writing – original draft. **Jeffrey T. Borenstein:** Supervision, Resources, Funding acquisition, Writing – review & editing. **Luis F. Velásquez-García:** Supervision, Resources, Funding acquisition, Writing – review & editing.

Declaration of Competing Interest

The authors declare that they have no known competing financial interests or personal relationships that could have appeared to influence the work reported in this paper.

Acknowledgements

The authors would like to thank Erin Maryzek, and Andy Dineen of Draper for consultations regarding and assistance with mechanical testing of materials.

Funding

This research is funded in part by the Draper Scholars Program.

Data availability

The raw/processed data required to reproduce these findings cannot be shared at this time due to technical or time limitations.

Appendix A. Supplementary data

Supplementary data to this article can be found online at https://doi.org/10.1016/j.mattod.2022.02.012.

References

[1] A.C. Backman, K.A.H. Lindberg, J. Mater. Sci. 36 (2001) 3777–3783, https://doi.org/10.1023/A:1017986119559.
[2] Bajaj, Y.P.S. (Ed.), 1991. Biotechnology in agriculture and forestry. 17. high-tech and micropropagation I, The Indian Journal of Genetics and Plant Breeding. Springer-V. https://doi.org/10.1007/978-3-642-76415-8.
[3] A.L. Beckwith, J.T. Borenstein, L.F. Velásquez-García, J. Clean. Prod. 288 (2021), https://doi.org/10.1016/j.jclepro.2020.125571 125571.
[4] F. Berthiaume, T.J. Maguire, M.L. Yarmush, Annu. Rev. Chem. Biomol. Eng. 2 (2011) 403–430, https://doi.org/10.1146/annurev-chembioeng-061010-114257.
[5] A.J. Bidhendi, Y. Chebli, A. Geitmann, J. Microsc. 278 (2020) 164–181, https://doi.org/10.1111/jmi.12895.
[6] M. Bologna, G. Aquino, Sci. Rep. 10 (2020) 1–9, https://doi.org/10.1038/s41598-020-63657-6.
[7] T.C. Browne, Cellul. Chem. Technol. 45 (2011) 455–460.
[8] O. Chaudhuri et al., Nature Mater 13 (2014) 970–978, https://doi.org/10.1038/nmat4009.

[9] M. Christiernin et al., Plant Physiol. Biochem. 43 (2005) 777–785, https://doi.org/10.1016/j.plaphy.2005.07.007.
[10] E. Cimetta, A. Godier-Furnémont, G. Vunjak-Novakovic, Curr. Opin. Biotechnol. 24 (2013) 926–932, https://doi.org/10.1016/j.copbio.2013.07.002.
[11] T.W. Crowther et al., Nature 525 (2015) 201–205, https://doi.org/10.1038/nature14967.
[12] L. Donaldson, N. Williams, Plants 7 (2018) 1–16, https://doi.org/10.3390/plants7010010.
[13] J. Emmermacher et al., Biofabrication 12 (2020), https://doi.org/10.1088/1758-5090/ab7553.
[14] H. Fukuda, A. Komamine, Plant Physiol. 65 (1980) 57–60, https://doi.org/10.1104/pp.65.1.57.
[15] A. Goldsworthy, K.S. Rathore, J. Exp. Bot. 36 (1985) 1134–1141, https://doi.org/10.1093/jxb/36.7.1134.
[16] V. Keriquel et al., Sci. Rep. 7 (2017) 1778, https://doi.org/10.1038/s41598-017-01914-x.
[17] J.P. Knox, 2012. In situ detection of cellulose with carbohydrate-binding modules, 1st ed, Methods in Enzymology. Elsevier Inc. .org/10.1016/B978-0-12-415931-0.00012-4.
[18] I. Perea-Gil, C. Prat-Vidal, A. Bayes-Genis, Stem Cell Res. Ther. 6 (2015) 248, https://doi.org/10.1186/s13287-015-0237-4.
[19] V. Placet, J. Passard, P. Perré, Maderas, Ciencia y tecnología 10 (2008) 45–60, https://doi.org/10.4067/S0718-221X2008000100005.
[20] J.C. Plomion, G. Leprovost, A. Stokes, Plant Physiol. 127 (2001) 1513–1523, https://doi.org/10.1104/pp.010816.
[21] S. Rocha et al., Front. Plant Sci. 5 (2014) 1–10, https://doi.org/10.3389/fpls.2014.00102.
[22] C. Schaller, Polymer Chemistry, Compiled 2. ed., LibreTexts, 2021.
[23] J. Seidel et al., Biofabrication 9 (2017) 045011, https://doi.org/10.1088/1758-5090/aa8854.
[24] A. Shrivastava, 2018. Introduction to Plastics Engineering. William Andrew Publishing. https://doi.org/https://doi.org/10.1016/B978-0-323-39500-7.00003-4.
[25] B.A. Simmons, D. Loque, H.W. Blanch, Genome Biol. 9 (2008) 242, https://doi.org/10.1186/gb-2008-9-12-242.
[26] N. Stephens et al., Trends Food Sci. Technol. 78 (2018) 155–166, https://doi.org/10.1016/j.tifs.2018.04.010.
[27] P. Twumasi et al., Cell Biol. Int. 33 (2009) 524–533, https://doi.org/10.1016/j.cellbi.2009.01.019.
[28] V. Vancauwenberghe et al., J. Food Eng. 263 (2019) 454–464, https://doi.org/10.1016/j.jfoodeng.2017.12.003.
[29] D. Weitz, H. Wyss, R. Larsen, GIT Lab. J. Eur. 11 (2007) 68–70.
[30] R. Wightman, C.J. Luo, Biochem. (Lond) 38 (2016) 32–35, https://doi.org/10.1042/bio03804032.
[31] I. Yu, S. Kaonis, R. Chen, Procedia CIRP 65 (2017) 78–83, https://doi.org/10.1016/j.procir.2017.04.020.